# Which Satellite Image should be used for Mapping

Jacobsen, K.

Institute of Photogrammetry and GeoInformation Leibniz Universität Hannover - jacobsen@ipi.uni-hannover.de

**KEY WORDS:** Topographic Mapping, Satellite Images, Orientation, Image Quality, Ground Resolution

**ABSTRACT:**

Today, topographical mapping based on satellite images is a standard method. With the large number of very high-resolution optical satellites, it only a question of the Ground Sampling Distance (GSD) and the map scale to be generated. But the classical large-format satellite images are expensive. With the today's variety of the classical small satellites (601kg to 1200kg) to Nano-satellites (1.1kg to 10kg) of 3U (10cm x 10cm x 30cm), various options are available that influence the economic solutions.

An overview of the accessible optical satellites is given, with some specific information on the mini-satellites that offer new economical solutions for topographic mapping. Significantly more optical satellites are currently in operation, but their images are used only for military purposes or they are restricted for national use due to lack of image storage and limited download possibilities.

## 1. INTRODUCTION

### 1.1 General

With SkySat, BlackSky, Jilin-1 and Nu-Sat, very high resolution optical imagery are available through constellations of inexpensive micro-satellites which are keen to capture market share from the large satellite systems such as from MAXAR and Airbus DS. According to European Copernicus project, Very High Resolution 1 corresponds to a GSD of 1m or less and Very High Resolution 2 corresponds to a GSD of more than 1m up to 4m.

This is not the first publication using SkySat imagery for mapping. Nevertheless, several publications are based on prototypes SkySat-1 and -2. With the launch of the SkySat C-series from September 2016, the ground resolution and also some technical components changed, and with the lowering of the orbit of SkySat-3 up to -15 from 500 km to 450km and the even lower orbit of SkySat-16 up to -21 of 400 km, the conditions are not what they were before. In addition, new image formats were created. These changes are at least partially ignored in the current internet information. With Planet's better ground resolution and also slightly improved data handling, we now have slightly better conditions than before.

### 1.2 Development of Space Images for Mapping

The use of satellite images for mapping started with analogue photos of CORONA KH-4A and KH-4B taken from 1963 up to 1972 (Jacobsen 2020). At first they were classified, but they are now available almost for free. This was followed in 1983 by the German Metric Camera Mission and in 1984 by the US Large Format Camera Mission from the Space Shuttle. The Hannover University was lucky to have access to the Russian space photos of the cameras KFA1000, KATE200, MK4, KFA3000, KVR1000 around 1990. The digital imagery from SPOT-1 to SPOT-4, launched from 1986 up to 1998, showed unsatisfactory detail for mapping with a GSD of 10m. The breakthrough came in 1999 with the civilian IKONOS with 0.81m GSD, initially reduced to 1m due to allowance restrictions. These restrictions from the USA have been gradually reduced from 1m over 50cm and 25cm to now 10cm for the ALBEDO satellite announced for 2024. Digital space images that can be used for mapping have been available since IKONOS in 1999. View direction flexibility allows in orbit stereo coverage, avoiding the side-view stereoscopic coverage time delay required by SPOT satellites. Once we ordered stereoscopic coverage from SPOT for an area near Hannover. The first image was taken in June and due to cloud coverage the second image was from July. In June the grain was green, in July it was yellow, preventing a stereo impression and image matching.

Since IKONOS came several digital optical satellites. The GSD for nadir view was reduced to 61cm for QuickBird, 41cm for Kompsat-2 and WorldView-2, 31cm for WorldView-3 and 30cm for Pleiades Neo. As already mentioned, Albedo is announced with 10cm GSD. It's not just the improved ground resolution, several steps have been improved. Today, the larger satellites are equipped with Control Moment Gyros (CMG), which allow the satellites to rotate one direction of view to the other faster than the former reaction wheels. The number of image pixels is increased, allowing a larger swath width. The data transmission from the satellites to the ground station is improved by additional ground stations or via a relay satellite. In addition, more images can be stored in internal storage. Instead of single satellites, satellite constellations are also active, which shortens the revisit time.

Several countries now operate optical Very High Resolution (VHR) satellites, such as initially only the USA and Soviet Union (Russia), followed by France, India, Taiwan, Israel, South Korea and later China. Today more than 25 countries operate their own VHR satellites. Some of the satellites were purchased in whole or in part from other countries.

The "ESA eoportal" https://www.eoportal.org/satellite-missions provides a comprehensive overview of the optical and radar satellites. Current short information is available at Orbital Launches https://space.skyrocket.de/doc_chr/lau2023.htm for the individual years.

The components of the optical satellites have become smaller and some can be bought off the shelf. This allows today optical micro-satellites (11kg to 100kg) or even nano-satellites with a size of 3U (1U = 10cm x 10cm x 10cm) or even just 1 U. This reduced the price including launch prices. Constellations of micro- and mini-satellites are now available e.g. 21 SkySats, 35


https://doi.org/10.5194/isprs-annals-X-1-W1-2023-827-2023 

NuSats, 14 BlackSky, and 53 Jilin-1, named also Daily Vision. These micro-satellites, weighting from 41kg to 120kg, provide images with 50cm to 1m GSD and can also choose the viewing direction. Of course, they have some reduced functions compared to the classic optical satellites, such as lower accuracy of the direct sensor orientation, slower slewing from one view direction to another and smaller swath width, but due to the lower price of the satellite, the images are distributed at lower cost. The situation is more extreme with the nano-satellites, they deliver images with 3m to 5m GSD. A typical example for this group are Planets Dove satellites. They are launched with large numbers, currently around 200 of them are in operation. Of course, they have limited lifespan of about 3 years, but they are not expensive.

### 1.3 Required ground sampling distance for mapping

Doyle (1984) published at first the relation between the scale of topographic maps and the required GSD as rule of thumb with: 0.1mm/pixel in the map scale, required for sufficient map contents. Based on several own tests with large number of different space and aerial images I modified this slightly to 0.05mm/pixel up to 0.1mm/pixel in the map with a limit of at least 5m required in any case also for very small map scales (Fig. 1).

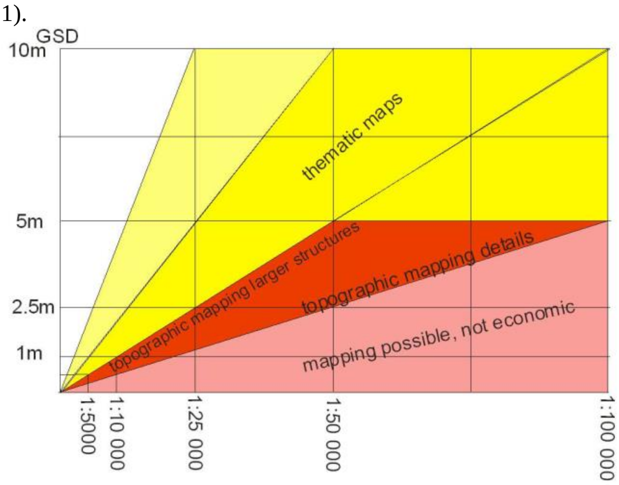


Figure 1: relation map scale to required GSD

According to this rule of thumb (red area in Fig. 1), topographic maps with a scale 1:10 000 can be generated with 1m GSD. In some countries, such as Switzerland, more details is show in the maps, with a 1: 10 000 topographic map requiring a GSD of 0.5m.

A typical mapping result is following shown on QuickBird images. This is of course not the newest satellite, but also typical for others.

The mapping test shown in Figure 2 shows that buildings can be mapped in images with 2.4m GSD – any building has been identified. But the details required for a larger map scale than 1:5000, including all building extensions, can only be identified in the image with 0.6m GSD. As a result of several mapping tests, the required GSD to identify the different objects as listed in Table I was found. Of course, as mentioned above, there are differences in object detail depending on the GSD used, but this confirms the above rule of thumb for the GSD in relation to the mapping scale.

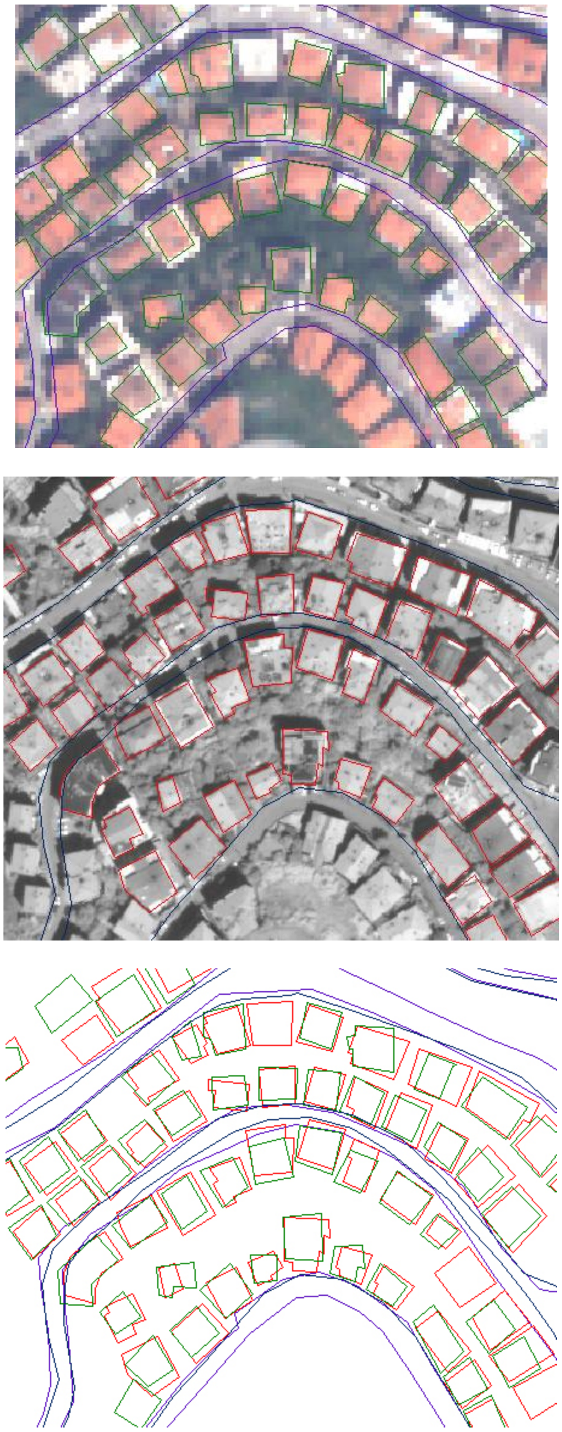

Figure 2: Top: mapping with QuickBird colour image (2.4m GSD), Centre: mapping with QuickBird panchromatic image (0.6m GSD), below: overlay of generated vectors (green for 2.4m GSD, red for 0.6m GSD)

| | required GSD |
|---|---|
| urban buildings | 2m |
| foot path | 1 - 2m |
| minor road network | 5m |
| rail road | 5m |
| fine hydrology | 5m |
| major road network | 10m |
| building blocks | 10m |

Table I: required GSD for topographic mapping


https://doi.org/10.5194/isprs-annals-X-1-W1-2023-827-2023 

### 1.4 Effective image resolution

The GSD is defined as the centre to centre distance between adjacent pixels projected onto the ground. This depends on the angle of incidence (nadir angle from the ground to the satellite) so it is only given for nadir viewing direction. The pixel size on the ground across the view direction corresponds to the pixel size in nadir direction divided by the cosine of the angle of incidence and in viewing direction it must be divided by the square of the cosine.

The geometric pixel size does not have to be equal to effective pixel size, important for object identification. At first it can be influenced by the atmosphere, but it also depends on the quality of the optical system. A simple investigation is possible by edge analysis.

A sharp grey value change in the object (Fig. 3 top left) can be seen smeared in the image (Fig. 3 bottom left). A differentiation of the grey value profile across the edge (Fig. 3 top right) leads to the point spread function (Fig. 3 bottom right). From the centre to the side at the turning tangent we have the factor for the effective resolution. Since the examination is performed with pixels, the factor for the effective resolution is normalized to the pixel size. A Factor 1.0 means that the image quality really corresponds to the geometric pixel size. Theoretically, this factor should not be less than 1.0, but can be influenced by image sharpening. A value above 1.0 means the effective image quality is not as good as it should be for the pixel size.

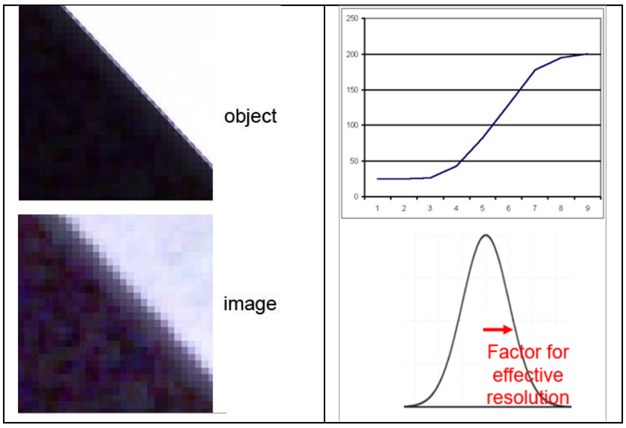


Figure 3: top left: grey value at an edge on ground, lower left: grey value distribution in the image, top right: grey value profile, bottom right: differentiation of the grey value = point spread function

## 2. IMAGE ORIENTATION

### 2.1 Analog Photos

Satisfactory orientation information that requires Ground Control Points (GCP) is not available for analogue space photos. By standard resection or by bundle block adjustment, in case of a strip or even a block of images, it has to be determined. The large format space images may have problems with systematic image errors that require self-calibration by additional parameters (Jacobsen 1990). Such systematic can be extreme in with panoramic cameras such as CORONA KH-4A and -4B (Jacobsen 2020). These images, which are now around 50 year old, can be helpful for special cases, such as determining the former location of moving watercourses, in order to identify positions where tall buildings should not be build today.

Identifying GCPs is time consuming and expensive. For smaller image scales it is satisfactory to use Google Earth as ground control information. In most cases, the standard deviation of Google Earth is a little under 2m. Of course, the geodetic datum of the national ground coordinate system relative to the International Terrestrial Reference Frame (ITRF) datum used by Google Earth must be known, and a transformation to a map projection other than UTM may be required. However, this problem becomes smaller due to the dominating use of GNSS positioning and a trend towards switching national maps to the UTM coordinate system in ITRF datum or a regional sub-version such as the European Datum ED50.

### 2.2 Digital images

The satellite images are currently supplied together with the direct sensor orientation in the form of Rational Polynomic Coefficients (RPC) (Grodecki 2001). The bottleneck of the direct sensor orientation is the rotation information. Through GNSS positioning, the location of the projection centre path is known accurately enough, but the gyro information used for the rotation elements only has high relative accuracy, but a drift that needs to be updated by star trackers. Still the big satellite companies like Maxar and Airbus DS have worldwide ground control information, which reduces this problem. But even with this not bad information, the RPC should be improved by bias correction with affine transformation to local GCP.

For IKONOS images, the RPC had to be purchased at great expense in the first few years. For this reason, some programs for image orientation of satellite line scanner images have been developed by universities and mapping institutions. In the Hannover University this was based on the given line of sight, the satellite altitude, orbit direction, the field of view and motion of the satellite together with ground control points, called geometric reconstruction. With 3 GCP, optimal near the corners of the image, the same accuracy as with the bias corrected RPC, also requires three GCP. Of course, over-determination is by at least one GCP is required for error detection. With this solution, the same accuracy as with the bias corrected RPC was achieved (Fig. 4) (Jacobsen 2006).

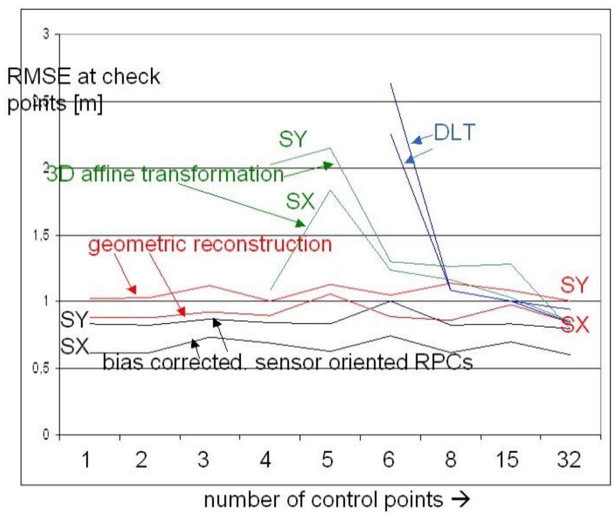


Figure 4: Standard deviation orientation of IKONOS, Zonguldak (mountainous); root mean square discrepancies at independent check points as function of GCP number - 32 GCPs = discrepancies at GCPs

Hanley, Yamakawa and Fraser (2002) used the approximation of a 3D-affine transformation to orientate satellite line-scanner images. The 3D-affine transformation requires GCP in 3D-distribution around the region of interest. In addition, there are accuracy limitations for larger scenes, which Jacobsen (2008) solved with some additional terms for 3D-affine transformation. Fig. 4 shows a typical relationship of different orientation methods for QuickBird images as a function of the number of GCP. The bias corrected RPC leads to almost the same result as the geometric reconstruction. The approximation by 3D-affine transformation is not bad, but does not reach the same level of accuracy. The results of the 3D-affine transformation with the additional terms is not shown in Fig.2 because of overlay with the geometric construction, but requires at least 8 GCP. The Direct Linear Transformation (DLT) also used cannot be accepted.

For the relationship between scene and object coordinates, a limited number of polynomial coefficients of the standard RPC-formulas (Grodecki 2001) can be calculated based on control points, called “terrain dependent RPC’s”. The number of unknowns chosen depends heavily on the number and distribution of the control points. Just by the residuals of the control points the effect of this method cannot be controlled. Some commercial programs that include this method do not use statistical checks for high correlations of the unknowns, making it very dangerous to handle correctly. The residuals can be small, but the results can be very bad, especially in areas outside the control points. Like DLT, this method should also be avoided (Jacobsen., Büyüksalih, Topan 2005).

### 2.3 Height models for ortho-images

A Digital Elevation Model (DEM) is required for the generation of ortho-images, as well as for the GCP. Based on the X-Y position, the height can be interpolated from the DEM. Currently, the SRTM elevation model, or a modification thereof, is used. The Shuttle Radar Topography Mission (SRTM) was performed in February 2000 by interferometric radar from the Space Shuttle. The resulting SRTM DEM was the first freely available nearly global elevation model with a homogenous accuracy satisfactory for multiple applications (Gesch et al. 2014). AW3D30, based on ALOS PRISM stereo models, has the best morphologic information, but the absolute height accuracy is not as good as for the TanDEM-X DEM (TDM90). For this reason, I improve AW3D30 by TDM90 – labeled as ZFIT in Figure 5. There is also the ASTER GDEM based on ASTER stereo models available for free, but it’s not as good as the SRTM DEM, for this reason it’s not shown (Jacobsen, Passini 2021).

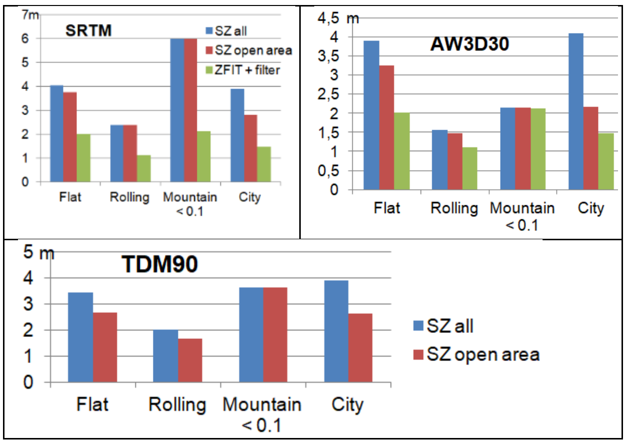


Figure 5: Standard deviations of SRTM, AW3D30 and TDM90 in relation to LiDAR for 4 different areas

All of these DEM are surface models with the height of the visible surface. For this reason, the overall accuracy and the accuracy in the open areas not disturbed by vegetation and buildings are shown in Fig. 5. The accuracy improved by the absolute accuracy of TDM90 is shown under ZFIT (green columns); filter means, it is filtered for elements that do not belong to ground level. In Fig. 4, note the different scales for the standard deviation in Z. Typical of the steep mountain terrain, the SRTM and TDM90s interferometric radar has some problems with foreshortening and layover. In the other areas, AW3D30 improved by TDM90 delivers the best result. The original SRTM data is not so good, especially in mountainous area (Jacobsen, Passini 2021)

## 3. MAPPING

### 3.1 3D-Mapping or 2D mapping

If there is only one image, only the direction from the projection centre to the object is given, which requires additional information. Usually this is the object height, available as DEM in most cases. It can be used to generate an ortho-image. Based on the ortho-image, a line map can be generated by on-screen digitizing. This is quite simpler than 3D-digitizing which requires a more experienced operator. Still, a very detailed DEM is required for accurate positioning - especially in build-up areas. The commonly used SRTM DEM should be replaced by AW3D30. In addition, the stereo effect supports the object identification and classification.

In some projects with different optical satellites, the 3D-line-mapping was compared with 2D-line-mapping from ortho-images. 2D-line mapping is easier for untrained staff. Very few classification errors were introduced by 2D-line-mapping when classifying parking lots in the row of buildings as houses. That didn’t happen with stereo mapping. Stereo-mapping has also the advantage of being more accurate than simple 2D-line-mapping, due to more precise location in undulated terrain and due to be independent on the DEM used for the ortho-image. It also simplifies object classification. Ultimately, choosing 3D- or 2D-mapping is a cost-benefit choice.

### 3.2 To be used type of satellite image

The most important characteristic for the selection of space images for topographic mapping is the GSD of the imagery. As mentioned above, a GSD of 0.05mm/pixel up to 0.1mm/pixel in the map with a limit of at least 5m is required in any case, even for very small map scales. This corresponds to a possible map scale of 1:5000 for 50cm GSD or 1:25 000 for 2.5m GSD. In addition, it is important to know if a stereo model is required or if a single image is satisfactory.

When details of the vegetation are required, the near infrared band is important. In the northern hemisphere, it may be of interest whether we have the leaf-on or leaf-off period for trees. For object classification – whether manual or automatic - colour information – at least red, green, blue (RGB) – is very helpful to absolutely necessary. In the early days of mapping with satellite imagery, we often only had panchromatic images and this sometimes caused problems in object recognition. Currently we have a trend towards extended colour information, as in WorldView-3 with 8 spectral bands from coastal blue to 2 bands in near-infrared with 1.24m GSD and 8 short-wave infrared (SWIR) bands with 3.7m GSD and 12 additional bands with 30m GSD. Also Pleiades Neo has 6 colour bands with 1.2m GSD instead of the usual 4 bands red, green, blue and near infrared

This contribution has been peer-reviewed. The double-blind peer-review was conducted on the basis of the full paper.
https://doi.org/10.5194/isprs-annals-X-1-W1-2023-827-2023 | © Author(s) 2023. CC BY 4.0 License. 

(RGBN). The coastal or deep blue band has better penetration of water and is used especially for depth survey of shallow water.

A stereo model is required to determine a DEM. Currently, most very high-resolution optical satellites are flexible, with a fast change in line of sight, which also allows for stereo or even three-stereo coverage in orbit. In the beginning this was based on reaction wheels, now more often control moment gyros. Reaction wheels are strap-down gyro combinations that apply a torque to the satellite if the gyros' rotation is accelerated or decelerated to change the direction of view. Control Moment Gyros (CMG) do the same thing, but the system is held in the same inertial orientation. With CMG, changing the direction of view is faster.

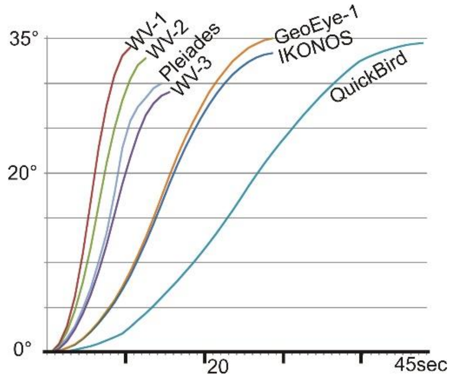

Figure 6: Slewing speed of some VHR satellites; vertical: change of the view direction [°], horizontal: required time

The slewing from one location to another starts at pointing to one position, followed by an angular acceleration, constant rotation and deceleration to the new position. Only newer large satellites are equipped with CMG. As shown in Fig. 6, the slewing speed is quite different. GeoEye-1, IKONOS and QuickBird are equipped with reaction wheels and rotate not as fast as the other equipped with CMG. QuickBird was slewing not fast enough to allow other imaging between the foreword view from one direction to an object up to the backword view to the same area. For this reason, stereo imaging with QuickBird was not economical. But the fast rotation can have a disadvantage of satellite jitter directly after slowing down the rotation to imaging mode. Jitter can affect the image quality and relative positioning in relation to object space, so a few seconds without angular rotation are required to avoid the jitter.

In general, the angle of incidence (nadir angle from the ground to the satellite) should not exceed 20°. Even more important than enlarged GSD is the reduced visibility of objects close to high objects. At larger angles of incidence, streets in build-up areas cannot be seen, as can objects near trees, and ortho-images require more accurate DEM.

| Angle of incidence | Pixel in view | Pixel across view |
|---|---|---|
| 10° | 1.02 m | 1.01 m |
| 20° | 1.11 m | 1.05 m |
| 30° | 1.26 m | 1.12 m |
| 40° | 1.55 m | 1.24 m |

Table II: Enlargement of 1m pixel in nadir view by angle of incidence

We currently have several VHR satellites that can be used for mapping. However, it is difficult to obtain images from several satellites due to missing or not optimal distribution system. The image distributor Satellite Imaging Corporation has a list of satellites for which images can be ordered (Table III). It does not include images of Russian satellites, they are not available on the market.

| satellite | Pan GSD | remark |
|---|---|---|
| Pleiades Neo | 0.30m | 2 satellites |
| SuperView-Neo | 0.30m | = GaoJing-1 |
| WorldView Legion | 0.30m | 6 satellites shall be launched |
| WorldView-3 and -4 | 0.30m | WV-4 ended 2019 |
| Göktürk-1 | 0.50m | |
| Worldview-1 and -2 | 0.50m | |
| GeoEye-1 | 0.50m | |
| Pleiades-1A and 1B | 0.50m | |
| SuperView-1 | 0.50m | = GaoJing-1 |
| KOMPSat-3 | 0.70m | |
| KOMPSat-3A | 0.55m | |
| QuickBird | 0.65m | Ended 2014 |
| Satellogic | 0.70m | |
| Gaofen-2 | 0.80m | |
| TripleSat | 0.80m | 3 satellites = Beijing-2 |
| IKONOS | 0.81m | Ended 2015 |
| SPOT-6 and -7 | 1.50m | |
| Mini satellites | | |
| SkySat | 0.50m | 21 Mini satellites |
| Daily Vision | 0.75m | =Jilin-1 53 satellites |

Table III: Satellites – images distributed by Satellite Imaging Corporation

Only four Chinese satellite types are included in table III. China has a high number of optical satellites, but mainly for internal use only. With the exception of the SkySat and Daily Vision micro satellites, the satellites in Table III are classic large satellites, that can rotate fast and can create stereo pairs in the same orbit. The mini satellites SkySat and Daily Vision (Jilin-1) are equipped with a CMOS matrix instead of CCD-lines or Transfer Delay and Integration (TDI) multi-line sensors. For a GSD below 2m, the exposure time is too short for the required image quality. So in case of a TDI, the charge generated in one pixel is shifted to the adjacent CCD-line according to the forward motion and more charge is added – this is repeated a number of times until a satisfactory charge is reached.

Edge analysis of images from most of the large optical satellites in table III confirmed the effective image quality corresponding to the nominal pixel size. This is also applies to the satellites where the physical GSD is larger than the distributed GSD – for example SPOT-6 and -7 have 2m physical GSD, but image processing reduces the distributed GSD to 1.5m.

The geometric property of the images captured by large satellites depends more on the quality of the GCP and check points used than on the satellites. Sub-pixel accuracy can be achieved with well-defined points, but mostly the accuracy is limited by identifying the points in the images.

| satellite | GSD | b/h | swath | remark |
|---|---|---|---|---|
| MOMS 2P | 6m | 1:1.3 | 50km | from MIR |
| SPOT-5 HRS | 5m | 1:1.9 | 120km | Only 200km |
| Terra ASTER | 15m | 1:2 | 60km | |
| Cartosat-1 | 2.5m | 1:1.6 | 27km | |
| ALOS PRISM | 2.5m | 1:1.0 | 35km | |
| TIANHUI-1 | 5m | 1:1.0 | 60km | |
| Ziyuan III-01 | 3.5m | 1:1.3 | 51km | |
| Ziyuan III-02 | 2.5m | 1:1.3 | 51km | |
| GaoFen-7 | 0.65m | 1:1.8 | | LiDAR profile |

Table IV: Stereo satellites


https://doi.org/10.5194/isprs-annals-X-1-W1-2023-827-2023 | © Author(s) 2023. CC BY 4.0 License.

Worldwide DEM cannot be generated from the flexible satellites listed in table III. Stereo coverage requires changing the view direction from the forward view to the backward view. Full stereo coverage is solved by stereo or even tri-stereo satellites equipped with 2 or 3 cameras (table IV). They can permanently image and cover long stereo strips. The only exception is SPOT-5 HRS. The stereo camera had 2 optics looking forward and backward but only one sensor for both. So after 200km flight, the sensor was switched from forward registration to backward registration. Nevertheless, SPOT-5 HRS was used for nationwide DEM generation. With Terra ASTER the almost worldwide ASTER GDEM was generated. Due to the GSD of 15m, this DEM is not as good as the almost worldwide ALOS World 3D (AW3D) based on ALOS PRISM with 2.5m GSD.

The mini satellites can also generate videos using the CMOS matrix. SkySat can produce videos at 30 Hz for 90 to 120 seconds. This high frame rate is also used to improve the quality of standard images. While each individually captured raw image frame is of moderate quality, ground-based image processing algorithms enhance the raw data by combining data from multiple frames to increase the image's signal-to-noise ratio and decrease the ground sample distance in a process called Skybox "digital TDI" (Murthy et al. 2014). The SkySsat Collect images are distributed with 50cm GSD based on the 81cm original GSD. By edge analysis the improved 50cm GSD images has been shown as justified. The SkySat configuration shall be followed by the Pelican configuration of Planet with a planned constellation of 32 satellites, for the generation of images with 30cm GSD.

Similar mini-satellite configurations are also available for NuSat with currently 39 satellites and 1m GSD and BlackSky with currently 14 satellites, also with 1m GSD. NuSat images are only directly downloaded, so NuSat offers building of customer owned ground stations, allowing frequent remapping.

### 3.3 SkySat Satellites

As an example of the potential of micro-satellites imagery, SkySat imagery has been investigated in detail. The basic idea behind SkySat was to build low-cost optical satellites to enable a larger constellation of satellites capable of providing very high-resolution imagery in a short period of time. A key factor of the SkySat-1 mission is the simplification of the spacecraft design and the use of ground-based image processing to achieve high system accuracy (Murthy et al. 2014).

With 120kg for SkySat-3 to -21, the satellites belong to the group of micro satellites (11 kg up to 200 kg) or SmallSats (under 600kg) (EOPortal Directory). Skysat-3 and the following have a propulsion system. This allowed SkySat-3 to SkySat-15 to reduce orbit altitude from 500km to 450km to improve ground resolution.

SkySat Satellites have one camera and within the focal-plane three staggered CMOS frames with panchromatic and multispectral halves. The three frames (Basic images) capture overlapping strips per satellite (ESA EDAP, 2021) (Fig. 7). The numbers in Figure 7 contain the focal plane number as first number, followed by the scene number of the data acquisition. As shown, the images from the three frame sensors do not line up in orbit direction. First of all, the focal plane numbers 12 and 15 differ due to the staggered arrangement of the frame sensors in the focal plane and due to the change of the orbit altitude from 500 km to 450 km, the relation of the imaged footprints also changed.

Each of the three frame sensors has 2560 x 2160 pixels, divided into 1080 pixels for the panchromatic channel and four times 250 pixels for RGBN.

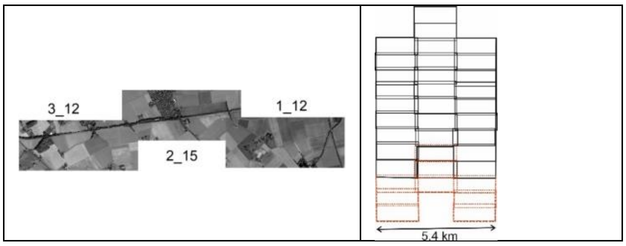

Figure 7: Left: Overlay of corresponding SkySat Basic images captured by the SkySat SSC12's three CMOS-frame sensors, right: arrangement of Basic images for SkySat Collect

The focal length of the camera is 3.6m. The pixel size corresponds to ~ 6.5µm. With this information, the orientation can be determined by resection in addition to the bias corrected RPC solution. Both methods provide the same level of accuracy, which can reach 1 pixel standard deviation with satisfying GCP.

| SkySat satellite | Orbit height | Geometric GSD | Covered area by Basic imagery |
|---|---|---|---|
| 3 – 15 | 450 km | 0.81 m | 2074 m x 875 m |
| 16 – 21 | 400 km | 0.72 m | 1843 m x 778 m |

Table V: Geometric ground sampling distance and area covered by SkySat Basic imagery as a function of flight altitude for the nadir view direction

Table V is based on a pixel size of 6.5 µm and 2560 x 1080 pixels. The GSD and the area covered are confirmed by the data sets used. As previously mentioned, in June 2020, SkySat-3 to -13 reduced the orbital altitude from 500 km to 450 km.

Image sharpening by the digital TDI is used for what is known as super-resolution, which reduces the GSD of the generated SkySat Basic Panchromatic (Table VI).

| Skysat satellite | Basic Panchromatic image | Basic Analytic (Multispectral image) |
|---|---|---|
| 1 – 2 | 0.86 m | 1.0 m |
| 3 – 15 | 0.65 m | 0.81 m |
| 16 - 21 | 0.58 m | 0.72 m |

Table VI: GSD of the Planet supplied images in nadir view

The GSD of the panchromatic images supplied by Planet (Planet Imagery Product Specification 2021) corresponds to a pixel size of 5.2 µm, i.e. the GSD is reduced by the factor 1.25 due to the super-resolution. The corresponding images have 3199 x 1349 pixels. Image sharpening is a common technique used also by other satellite imagery providers. Based on the configuration of the 3 adjacent Basic images and with a free number of image combinations in flight direction (Fig. 7 right), joint together in the form of ortho-images, are called SkySat Collect with distributed 0.50 m GSD.

In my own investigation, only images from SkySat-3, SkySat-9 and SkySat-14 (SSC1, SSC7 and SSC12) were used, which showed no differences in image quality.

(Aati and Avouac 2020) generated DEMs based on block adjusted neighboured SkySat Basic scenes using tie points with height constraint to a reference DEM. Based on LiDAR reference, a standard deviation in height of 3.9 m was achieved.

This shows the possibility, but it is not an economical solution due to the small image size.

To keep costs and weights down, the Skysat satellites were not designed to offer the best direct geo-referencing performance. (Smiley et al. 2014) from the SkyBox company (now Planet) mentioned that ground processing is far cheaper than star trackers. Despite this, the SkySat satellites are equipped with two 90 gram ST 15 star trackers and TQ 15 torque rods (Dzamba, 2014), but angular pointing accuracy is still limited. An investigation of an image strip of 37 Basic images resulted in root mean square differences of the orientations in X of 35 m and in Y (near the flight direction) of 65 m. In another strip of 12 Basic images, the root mean square differences are 44 m and 123 m, respectively. This is not satisfactory for mapping purposes and requires separate orientations for any Basic image.

Due to the small area covered, the use of non-optimal GCPs could not be avoided for the orientation. For 37 Basic Analytic scenes with 0.81m GSD, based on angles of incidence of 4° up to 6°, in the average the root mean square error (RMSE) of orientation in X is 1.16 m and in Y 1.01 m. The standard deviation, which corresponds to 1.3 pixels, is dominated by the uncertainty of the GCPs and less by the geometry of the images. Planet did the same by automatic matching to the same reference ortho that I used. Planet achieved an RMSE for X of 1.51 m and for Y 1.02 m based on several tie points per Basic image, with images having an angle of incidence less than 16.1°. The slightly lower accuracy in X can be explained by the influence of images with larger angle of incidence.

The RPC orientations of SkySat Basic Analytic images acquired at an incidence angle of 18° resulted in a standard deviation for X of 2.7 m and for Y of 1.3m. The X-direction is approximately in the view direction with a GSD of 0.90 m, the GSD in the Y-direction is 0.85 m. This corresponds to a standard deviation for X of 3 GSD and for Y of 1.5 GSD demonstrating the strong influence of the angle of incidence. No general differences could be determined between the images used from the different SkySat satellites.

CMOS- or CCD-sensors have a very high internal accuracy. However, due to the super resolution used in scene reconstruction, systematic discrepancies can also occure. Image deformations may be possible due to the optical system. Image distortions are not common with optics with such a small field of view – this has been confirmed by own investigation.

The lateral overlap of the three CMOS arrays is in the range of 5% to 7%. At 5% overlap, the total swath of images taken from 450 km orbit altitude is 7223 pixels for 0.81 m GSD, which corresponds to 5780 m for nadir view direction. Due to the situation that the nadir angle usually is across orbit, at 5° angle of incidence the swath is 5820 m, at 10° angle of incidence 5960 m and at 20° angle of incidence 6550 m. At SkySat-16 to -21, with an orbit height of 400 km, the swath is 11% smaller.

Triangulation with tie points between neighbouring SkySat Basic scenes is difficult due to the small overlap and large areas with unchanged texture. Due to this problem, Planet generated in the investigated project area SkySat Collect scenes by individual orientation of Basic Imagery in relation to an aerial ortho-image used as reference. Planet creates ortho-images of the Basic scenes and stitches the ortho-images together, also paying attention to misfits of neighbouring ortho-images.

Some SkySat Collect scenes were checked against the reference aerial ortho-image by manual identification of check points (Table VII).

| scene | Inci-dence | RMSX [m] | RMSY [m] | Bias X [m] | Bias Y [m] | SX [m] | SY [m] |
|---|---|---|---|---|---|---|---|
| 1 | 3.7° | 3.19 | 1.27 | 2.48 | 0.47 | 2.00 | 1.18 |
| 2 | 4.3° | 2.55 | 0.90 | 2.04 | -0.31 | 1.52 | 0.84 |
| 3 | 9.3° | 2.02 | 1.94 | -0.71 | 0.87 | 1.89 | 1.73 |
| 4 | 16.6° | 1.81 | 1.17 | 1.14 | 0.53 | 1.14 | 1.05 |
| 5 | 16.7° | 1.44 | 1.04 | 0.81 | 0.24 | 1.20 | 1.02 |
| 6 | 25.2° | 4.35 | 2.73 | 3.13 | -2.02 | 3.03 | 1.83 |
| 7 | 30.8° | 5.97 | 3.12 | 4.31 | 1.76 | 4.13 | 2.51 |
| 8 | 33.6° | 5.46 | 3.25 | 4.30 | 1.13 | 3.36 | 3.05 |
| 9 | 37.8° | 9.92 | 4.28 | -6.28 | 1.78 | 7.68 | 3.89 |

Table VII: Accuracy numbers of SkySat Collect images

Table VII clearly shows the dependency of the accuracy – RMS, bias and standard deviation - from the incidence angle. This becomes clearer in the graphical presentation in Fig. 7.

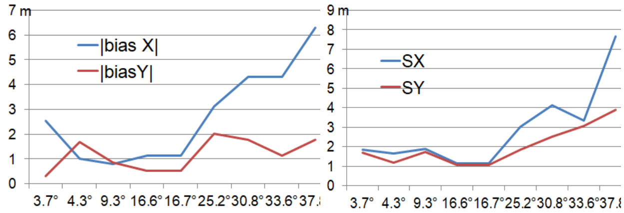


Figure 7: Absolute value of bias and standard deviation of SkySat Collect geo-reference as function of angle of incidence

The result of the SkySat Collect investigation is unequivocal, above an incidence angle of 20° the geo-reference accuracy of 4m required for the project was not achieved. First, the GSD is increased by an average of 10% at 20° angle of incidence, but more importantly, data sets 6 through 9 are not in flat area like the others, they are in the Sauerland, a gentle mountainous area with high proportion of forest. In the forest area, the matched reference points from the reference orthoimage are located on the canopy, which leads to systematic errors (bias) which is the dominant problem, especially in the X-direction. The X-direction is close to the view direction. However, systematic errors also play an important role in the areas with angles of incidence below 20° (data set 1 - 5). Modified and new buildings had to be identified in the project. The automatic building detection is based on roofs. At an angle of incidence of 20°, the roof of a 5m high building will shift by 1.8 m, which must be taken into account. The usability of SkySat images to update building information for German cadastre has been confirmed. The economic conditions show advantages for this project of only horizontal mapping for the use of SkySat Collect imagery over aerial and very high resolution classical satellite imagery.

## 4. CONCLUSION

The dominating factor affecting the scale of topographic maps generated from optical satellite images is the GSD. The rule of thumb of required 0.05 up to 0.1mm/pixel in the map scale was confirmed. For a topographic map 1:5000, a ground pixel size of 0.5m GSD is necessary. The required horizontal accuracy of topographic maps varies, but usually it is between 0.2mm and 0.5mm in the map. With a 1:5000 map, this corresponds to 1m up to 2.5m, or in the relation to above rule of thumb to 2 up to 5 pixels. All the VHR optical satellites listed in table III can be used according to their GSD.

The images of the mini-satellites are usually cheaper in relation to the covered area than images of the large satellites, so the question arises as to which satellite offers the most economical conditions. Direct use of the SkySat Basic images can only be suggested for very small projects where 3D-mapping is not required due to the time-consuming geo-reference information required. DEM by theory can be generated with Basic imagery, but this is not economical. For 2D-mapping, SkySat Collect images can be an optimal solution due to geo-reference with a standard deviation below 4m. As shown in Tab. VII and figure 7, for incidence angles below 20°, even approximately 2m is reached. Of course, also the large format optical space images provide good results for 2D-mapping, even with higher horizontal accuracy, but it is questionable if the higher cost justifies this. In conclusion, microsatellite configurations have been dominated by the fast information content, but they also open up new possibilities for mapping purposes. Also for the large optical satellites, the revisit time was improved by satellite configurations like Pleiades Neo, for which 4 identical satellites were planned, but the launch of the last 2 satellites failed. For the WorldView Legion 6 identical satellites are planned. China also has satellite constellations, but up to far they are more for internal Chinese use, with the exception of the 53 Daily Vision (Jilin-1).

The nano-satellites, like the Flock configuration with about 200 active satellites, offer also some cheaper options, but the 3m to 5m GSD is just enough for the 1 : 50 000 map scale. Here the object change detection for map update required is possible. However, with the exception of the larger constellations, most of these small satellites are for internal use only and have no distribution system.

In conclusion, it can be stated, that the classic large format optical satellites and the small satellites have their field for application. With both, we now have more options for economical topographical mapping. One group will not replace the other, both have their place.

## REFERENCES

Aati, S., Avouac J.-P., 2020. Optimization of Optical Image Geometric Modeling, Application to Topography Extraction and Topographic Change Measurements Using PlanetScope and SkySat Imagery, Remote Sensing 2020, 12, 3418

Doyle, F.J., 1984: Surveying and Mapping with Space Data, ITC Journal 1984

Dzamba, T. Enright, J., Sinclair, D., Amankwah, K., Votel, R., Jovanovics, I., McVittie, G.R.., 2014: Success by 1000 improvements: Flight Qualification of the ST-16 Star Tracker. In: 28th Annual AIAA/USU Conference on Small Satellites.

eoPortal Directory: https://www.eoportal.org/satellite-missions (Apr. 2023)

ESA EDAP: Technical Note on Quality Assessment for Skysat, 2021, https://earth.esa.int/eogateway/documents/20142/37627/EDAP.REP.015+TN+on+Quality+Assessment+for+SkySat_v1.0.pdf/59a2a91d-eecd-20f1-4a13-e670dad8eed3 (Apr. 2023)

Gesch, D.B., Oimoen, M.J.,Evans, G.A., 2014. Accuracy assessment of the US Geological Survey National Elevation Dataset, and comparison with other large-area elevation data sets: SRTM and ASTER, https://pubs.usgs.gov/of/2014/1008/pdf/ofr2014-1008.pdf

Grodecki, J. 2001: Ikonos Stereo Feature Extraction - RPC Approach, ASPRS annual convention, St Louis 2001

Jacobsen, K., 1990: Cartographic Potential of Space Images, ISPRS Com II Dresden 1990, Int. Arch. Photogramm. Remote Sens. Spatial Inf. Sci., Commission II, Dresden 1990, pp 127-134

Hanley, H.B., Yamakawa. T., Fraser, C.S., 2002: Sensor Orientation for High Resolution Imagery, Pecora 15 / Land Satellite Information IV / ISPRS Com. I, Denver

Jacobsen, K., 2002: Mapping with IKONOS images, EARSeL, Prag 2002“Geoinformation for European-wide Integration” Millpress ISBN 90-77017-71-2, pp 149 – 156

Jacobsen. K., Büyüksalih, G., Topan, H., 2005: Geometric Models fort the Orientation of High Resolution Optical Satellite Sensors, Int. Arch. Photogramm. Remote Sens. Spatial Inf. Sci., Vol. XXXVI-1/W3

Jacobsen, K, 2006.: Pros and cons of the Orientation of very high Resolution Optical Space Images, ISPRS Com I, Paris 2006, IntArchPhRS. Vol XXXVI Part 1

Jacobsen, K., 2008: Satellite image orientation, International Archives of Photogrammetry, Remote Sensing and Spatial Information Sciences, Vol. XXXVII, Part B1 (WG I/5) pp 703-709

Jacobsen, K., 2020: Calibration and Validation of CORONA KH-4B to Generate Height models and Orthoimages, ISPRS Annals Photogramm. Remote Sens. Spatial Inf. Sci., V-1-2020, 151–155, 2020

Jacobsen, K., Passini, R., 2021: Analysis and Bias Improvement of Height Models based on Satellite Images, Int. Arch. Photogramm. Remote Sens. Spatial Inf. Sci., XLIII-B1-2021, 23–30, 2021

Murthy, K., Shearn, M., Smiley, B., Chau, A., Levine, J., Robinson, D., 2014. SkySat-1: very high-resolution imagery from a small satellite, Proc. SPIE 9241, Sensors, Systems, and Next-Generation Satellites XVIII, 92411E (7 October 2014)

Planet Imagery Product Specification Febr. 2021. https://assets.planet.com/docs/Planet_Combined_Imagery_Product_Specs_letter_screen.pdf

Smiley, B., Levine, J., Chau, A., 2014: On-Orbit Calibration Activities and Image Quality of SkySat-1, JACIE 2014.